MECHANICAL RESPONSE OF AN EXTENDED CYCLIC PLASTICITY MODEL UNDER MULTI-STEP VARIABLE AMPLITUDE LOADING CONDITION

TSUTSUMI Seiichiro*

Abstract

The mechanical behavior of materials under variable amplitude loading conditions is a problem of great interest, since the stress often deviates severely from constant amplitude in many real situations. For the description of the cyclic loading behavior observed during the so-called high-cycle fatigue subjected to the cyclic stresses lower than the yield stress, a cyclic plasticity model was proposed by the authors. This paper is dedicated to the understanding of the mechanical response of the plasticity model under not only constant but also multi-step variable amplitude loading conditions.

KEY WORDS: (plasticity), (fatigue), (cyclic softening), (constitutive model), (damage)

1. Introduction

The mechanical behavior of materials under variable amplitude loading conditions is a problem of great interest, since the stress often deviates severely from constant amplitude in many real situations. On the other hand, the yield stresses of steels are often prescribed by the experimental stress-strain curves under monotonic loading conditions exhibiting the linear elastic, the upper/lower yielding, the plateau and the hardening responses, whilst a smooth elastic-plastic transition has been observed reaching toward the dominant yielding state (c.f. [1], [2]). This kind of linear/elastic response under a certain lower-stress level than the dominant yielding stress is widely observed not only under monotonic but also under cyclic loading conditions up to a certain number of cycles, so-called macroscopically elastic stress state, in which plastic strain is not observed macroscopically. So, in the conventional elastoplastic model, the yield surface for such materials is determined based on the dominant yield stress, and the inside of yield surface is assumed to be a purely elastic state. In other words, the plastic strain is induced only after satisfying the dominant yield condition, and then any plastic strain is not predictable under macroscopically elastic condition.

However, the fatigue failure of steels could be apparently induced, even if all stress amplitudes never exceeded the macroscopic yield stress. Some elaborated fatigue experiments, that focused on the damage accumulation observed in the stress-strain relationships under macroscopically elastic condition, have revealed that the plastic stain is suddenly generated after a certain number of cycles, which might be interpreted as cyclic softening. To understand and evaluate the fatigue processes of materials, appropriate descriptions of the cyclic plasticity responses would be required, and then various models have been proposed up to the present (c.f. [3]-[8]). These and extended models are categorized in the framework of unconventional plasticity premising that an interior of the yield surface is not the elastic domain [9]. These models, however, are originally designed for the simulation of fatigue process of materials under relatively larger stress amplitude than the macroscopic yield (or elastic limit) stress, which leads to low- or extremely low-cycle fatigue. The unconventional plasticity model describing the cyclic loading behavior of metals not only under macroscopic yielding but also under macroscopically elastic condition is proposed by the authors ([10]-[17]). The model is based on an elastoplastic constitutive model adopting a subloading surface concept and extended by incorporating the concepts of the elastic boundary and the cyclic damage together with the consistent material functions. The proposed model exhibits a purely elastic

† Received on December 17, 2012
* Associate Professor, JWRI, Osaka University

Transactions of JWRI is published by Joining and Welding Research Institute, Osaka University, Ibaraki, Osaka 567-0047, Japan

response under particular lower state of stress, a smooth elastic-plastic transition and a sudden generation of plastic strain keeping the mechanical features of the original model. In this article, the mechanical responses of the unconventional plasticity model describing the cyclic loading behavior of metals is examined under multi-step variable amplitude loading condition.

2. Outline of cyclic plasticity model

The extended cyclic plasticity model of metals is reviewed here. Drucker [9] defined unconventional elastoplasticity as the extended elastoplasticity such that the interior of the yield surface is not a purely elastic domain, but a plastic deformation is induced by the rate of stress inside the yield surface. In this study the subloading surface model, which falls within the framework of unconventional elastoplasticity, is adopted.

2.1 Stretching and Stress Rate

Denoting the current configuration of the material particle by x and the current velocity by v, the velocity gradient is described as $\mathbf{L} = \partial \mathbf{v} / \partial \mathbf{x}$ in which the stretching and the continuum spin are defined as $\mathbf{D}$ ($=(\mathbf{L}+\mathbf{L}^{\mathrm{T}})/2$) and W ($=(\mathbf{L}-\mathbf{L}^{\mathrm{T}})/2$), respectively, where $(\ )^{\mathrm{T}}$ stands for the transpose. In this study, the stretching $\mathbf{D}$ is additively decomposed into elastic stretching $\mathbf{D}^e$ and plastic stretching $\mathbf{D}^p$, i.e.

$$\mathbf{D} = \mathbf{D}^e + \mathbf{D}^p, \quad \mathbf{D}^e = \mathbf{E}^{-1}\overset{\circ}{\boldsymbol{\sigma}} \tag{1}$$

where $\boldsymbol{\sigma}$ is the Cauchy stress. $(\circ)$ indicates the proper corotational rate with the objectivity and the fourth-order tensor E is the elastic modulus.

2.2 Normal-yield and subloading surface

In the subloading surface model [8], the conventional yield surface is renamed the normal-yield surface, since its interior is not regarded as a purely elastic domain. Then, let the subloading surface be introduced, which always passes through the current stress point and also keeps the shape similar to the normal-yield surface and the orientation of similarity to the normal-yield surface with respect to the origin of the stress space. The similarity and orientation of similarity of these surfaces possess the following geometrical properties. All of the ratios of length of an arbitrary line element connecting two points inside the subloading surface and that of an arbitrary conjugate line-element connecting two conjugate points inside the normal-yield surface, are identical. The ratio is called the similarity ratio which coincides with the ratio of the sizes of these surfaces. Let the similarity ratio of the subloading surface to the normal-yield surface be called specifically the normal-yield ratio, and let it be denoted by R, where R=0 corresponds to the null stress state, 0<R<1 to the sub-yield state and R=1 to the normal-yield state in which the stress lies on the normal-yield surface. Therefore, the normal-yield ratio R plays the role of a three-dimensional measure of the degree of approach to the normal-yield state.

The subloading surface is given by

$$f(\overline{\boldsymbol{\sigma}}, \mathbf{H}) = RF(H), \tag{2}$$

where

$$\overline{\boldsymbol{\sigma}} \equiv \boldsymbol{\sigma} - \overline{\boldsymbol{\alpha}} \ (= R\,\hat{\boldsymbol{\sigma}}), \quad \overline{\boldsymbol{\alpha}} \equiv \mathbf{s} - R(\mathbf{s} - \boldsymbol{\alpha}), \tag{3}$$

where $\overline{\boldsymbol{\alpha}}$ on or inside the subloading surface is the conjugate point of $\boldsymbol{\alpha}$ on or inside the normal-yield surface. F is the isotropic hardening/softening function. The scalar H and the tensor H are the isotropic and the anisotropic hardening variables, respectively. The function f is assumed homogeneous of degree one in the stress. Then, if H= const., the yield surface keeps a similar shape. The normalized outward-normal at the current stress on the subloading surface is represented by N. The second-order tensor $\boldsymbol{\alpha}$ is the so-called back-stress which plays the role of the kinematic hardening variable as it translates with the plastic deformation. The kinematic hardening of the normal yield surface describes the Bauschinger effect characterized by early re-yielding, which is mainly due to the motion of less stable dislocations, such as piled-up dislocations.

2.3 Elastic boundary surface and smooth elastic plastic transition

It is well known for many metallic materials that an elastic response, such as Hooke's type, would be observed under a particular lower state of stress, so-called proportional or elastic limit. Even though, we should note that material responses also exhibit a smooth elastic-plastic transition with the increase of stress to the dominant yielding state.

Following these facts the subloading surface model, categorized in the unconventional plasticity model and describing a smooth elastic-plastic transition, is extended to describe an elastic response. Here it should be noted that the terminologies of "proportional" or "elastic limit" are often used in an obscure style, both of which are not representing a purely elastic response of materials itself, since the former one guarantees only a proportionality of stress-strain relation and the later is often defined in engineering sense as the minimum stress inducing a particular amount of measured small inelastic strain.

Now, the concept of the elastic boundary is introduced, in which the elastic response is assumed under the following condition:

$$f(\overline{\boldsymbol{\sigma}}, \mathbf{H}) \leq R^e F(H). \tag{4}$$

R^e is a material function of the stress and the plastic internal variables in general, which controls the size of the elastic boundary surface (see. **Fig**. 1). For the purpose of describing a smooth elastic-plastic transition, the evolution rule of the similarity-ratio R is given by

$$\dot{R} = mU \,\|\mathbf{D}^p\| \ (\mathbf{D}^p \neq \mathbf{0}). \tag{5}$$

m (>0) is a material constant prescribing the approaching rate of the current stress to the normal-yield surface. The function U in Eq. (5) is required to satisfy the following relations:

$$U = \begin{cases} +\infty & \text{for } R = R^e, \\ 0 & \text{for } R = 1, \end{cases} \quad (U < 0 \quad \text{for } R > 1). \quad (6)$$

U is assumed to be a monotonically decreasing function of R. The function U satisfying the relation of Eq. (6) is given in this study as

$$U = -(1-D)\ln\frac{R-R^e}{1-R^e}, \quad (7)$$

where the damage function D, as will be explained later, is introduced to represent the magnitude of the accumulated damage in the material. In the case of R^e =0 the model results in the conventional subloading surface model without a pure elastic response. On the other hand, the model with R^e =1 falls within the framework of conventional plasticity without a smooth elastic-plastic transition. In case of the R>1, a stress is automatically drawn back to the normal-yield surface since it is formulated that U>0 for R<1 (sub-yield state) and U<0 for R>1 (over the normal-yield state). The stress is controlled so as to approach automatically to the normal-yield surface in the plastic-loading process.

2.4 Cyclic damage counting

Various phenomena of deformation process, like hardening/softening material behavior, formation of shear bands and void/crack evolution, are very sensitive to a change of the deformation path at both macro- and micro-level. A physically justified description of a progressive degradation of the mechanical properties of solids under loading histories, attributed to the accumulated damage, is the central problem of resent constitutive descriptions in mechanics. In this study the concept of cyclic damage is introduced so as to describe the increase of the inelastic stretching due to the accumulation of plastic deformation during cyclic loading. Let the function D representing the magnitude of the accumulated damage in a material is introduced. For the purpose of describing a smooth evolution and a saturation behavior of the accumulated damage, the cyclic damage function D incorporated in Eq. (7) is assumed to be given as

$$D(d_i, H_d) = (1-d_2)\{1+(\frac{d_1}{H_d})^{d_3}\}^{-1}, \quad (8)$$

where d_1, d_2 and d_3 are material constants. H_d is a scalar-valued plastic internal variable, which is called the damage parameter and represents the magnitude of accumulated damage such as the accumulated plastic strain or plastic work. As can be seen from **Fig**. 3, with the increase of the damage parameter H_d, the value of D increases from 0 and saturates for the value of $1-d_2$.

Based on the equations formulated in the previous section, the constitutive equation for metals will be formulated. Let the Mises type of loading function f for the subloading surface be given for plastically incompressible metals as

$$f(\bar{\boldsymbol{\sigma}}) = \sqrt{\frac{2}{3}}\,\|\bar{\boldsymbol{\sigma}}^*\|, \quad \bar{\boldsymbol{\sigma}}^* \equiv \bar{\boldsymbol{\sigma}} - \frac{1}{3}\mathrm{tr}(\bar{\boldsymbol{\sigma}})\mathbf{I}. \quad (9)$$

The kinematic hardening is expressed by the translation of the normal-yield surface with the plastic deformation. The translation rule of the center of the normal-yield surface is assume to be given by

$$\overset{\circ}{\boldsymbol{\alpha}} = a_1 (a_2 \frac{\bar{\boldsymbol{\sigma}}^*}{\|\bar{\boldsymbol{\sigma}}^*\|} - \boldsymbol{\alpha})\{1+(\frac{F_0}{\|\bar{\boldsymbol{\sigma}}^*\|})^{a_3}\}\,\|\mathbf{D}^p\|, \quad (10)$$

where a_1, a_2 and a_3 are material constants.
The translation rule of the similarity-center is assumed as follows:

$$\overset{\circ}{\hat{\mathbf{s}}} = -c(1-D)\,\|\mathbf{D}^p\|\,\tilde{\boldsymbol{\sigma}} + \overset{\circ}{\boldsymbol{\alpha}} - \hat{\mathbf{s}}, \quad (11)$$

where c is a material constant, influencing the translating rate of the similarity-center.
The concept of the damage is introduced to describe a progressive degradation of the mechanical properties of metals attributed to the accumulated damage. For the purpose of describing a smooth evolution and a saturation behavior of the damage, the rate form of the damage parameter H_d is given by

$$\dot{H}_d = \sqrt{\frac{2}{3}}\,\|\mathbf{D}^p\|\,\bar{D}(k_i, \bar{R})$$

$$\bar{D}(k_i, \bar{R}) = (1-k_2)\{1+(\frac{k_1}{\bar{R}})^{k_3}\}^{-1}$$

$$\bar{R} = R - R^e, \quad k_1 = \frac{1-R^e}{2} \quad (12)$$

where k_2 and k_3 are material constants. In the case of D=0, the model results in the subloading surface model with the elastic boundary concept but without the damage effect.

3. Mechanical responses under single-step loading condition

The mechanical behavior of the proposed model is examined in this section. Fig. 1 shows the stress-strain relation calculated by the proposed model under monotonic tension condition, selecting material parameters as follows:

$E = 206$ (GPa), $\nu = 0.3$, $F_0 = 350$ (MPa),
$R^e = 0.4$, $m = c = 20000$,
$a_1 = 0.75$, $a_2 = 750$(MPa), $a_3 = 4$,
$d_1 = 0.0035$, $d_2 = 1.6$, $d_3 = 0.0055$,
$k_2 = 8$, $k_3 = 0.5$.

As shown in Fig. 1, the calculated results exhibit a smooth elastic-plastic transition of stress-strain relation. Next the performance of describing mechanical response to the cyclic stress lower than yield stress is examined. The definitions on the mechanical parameters can be given as follows, (i) The net cyclic plastic strain range $\Delta\varepsilon^p$ at zero stress level, (ii) The accumulated cyclic

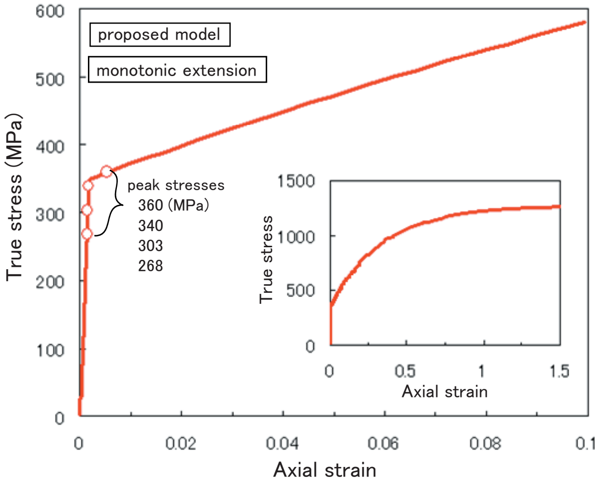

Fig.1 Stress-strain relation predicted by the proposed model under monotonic extension loading

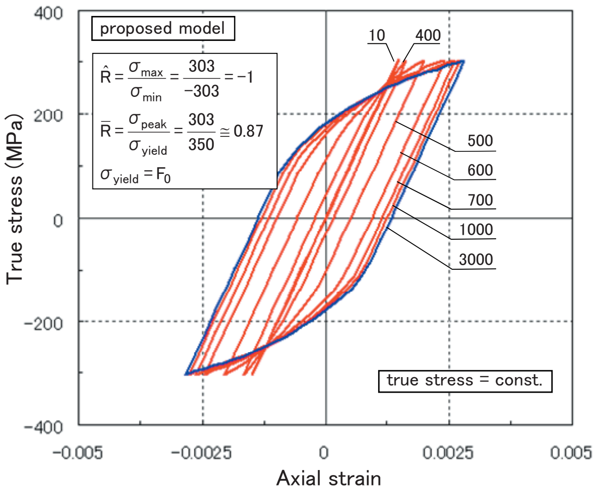

Fig.2 Stress-strain curve under symmetrical cyclic loading

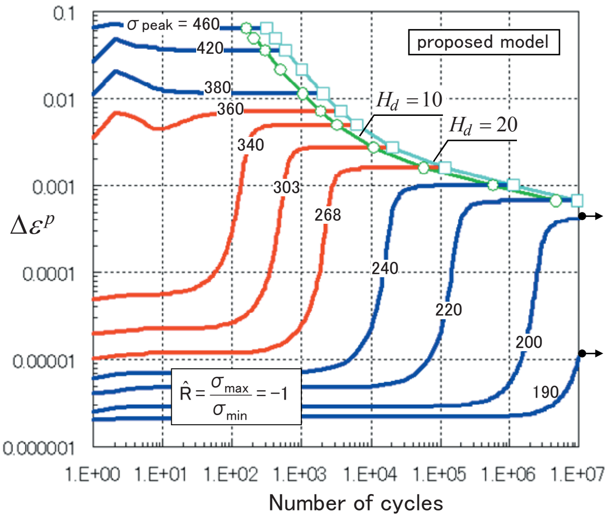

Fig.3 Evolution of plastic strain range with the increase of number of cycles

plastic strain $\bar{H}$ ($=2\sum\Delta\varepsilon^p$), and (iii) The center of cyclic loop $\bar{\varepsilon}$.

The symmetrical cyclic loadings with a prescribed peak true stresses are applied. **Fig.** 2 shows the calculated result of the true stress-strain relations at the particular number of cycles. As can be seen from this figure, when the number of cycles reaches around 400, the net cyclic plastic strain ranges $\Delta\varepsilon^p$ begin to increase rapidly. Furthermore, the burst of the net cyclic plastic strain ranges $\Delta\bar{\varepsilon}^p$ is accelerated up to around 600 times, whilst $\Delta\varepsilon^p$ stops to increase at around 1000 times. The mechanical parameters $\Delta\varepsilon^p$, $\bar{H}$ and $\bar{\varepsilon}$ under these circumstances are plotted against the number of cycles in **Fig**. 3. As can be seen from this figure, the strain parameter $\Delta\varepsilon^p$ evolves with the increase of number of cycles for the wide range of the prescribed cyclic stresses. From these figures we can find that the proposed model has capability of predicting experimental evidences for cyclic loading behaviors under macroscopically elastic conditions.

4. Mechanical responses under multi-step variable amplitude loading condition

Now, the mechanical response under multi-step changes of applied stresses is calculated. The following two stress histories (Case 1, 2) are applied under symmetric loading condition with the periodic changes for three types of peak stresses (σa=268, 303 and 340 MPa) at every 1000 cycles;

Case 1)
±303 → ±340 → ±303 → ±268 →±303 (MPa)
Case 2)
±303 → ±268 → ±303 → ±340 →±303 (MPa)

Figs. 4 and 5 show the results on the evolutions of plastic strain range and damage parameter with the increase of number of cycles under multi-step changes of symmetrical cyclic stresses until H_d =10, for the Case 1 and 2, respectively. The predicted number of cycles to H_d =10 for the Case 1) and 2) was $N^{case1)}$ =7847 and $N^{case2)}$ =7991, respectively. These results reflect the nonlinearity of material response, i.e. the stress and history dependency on the damage accumulation. Further numerical studies and experimental tests should be conducted to discuss deeply the applicably of the proposed model.

5. Concluding Remarks

The proposed cyclic plasticity model captures several important features of the behavior of metals under cyclic loading, e.g. hysteresis loop, cyclic softening and cyclic stress-strain curve. The model is based on the subloading surface model and extended by incorporating elastic boundary and cyclic damage concepts. In this paper, the mechanical responses under cyclic loading conditions

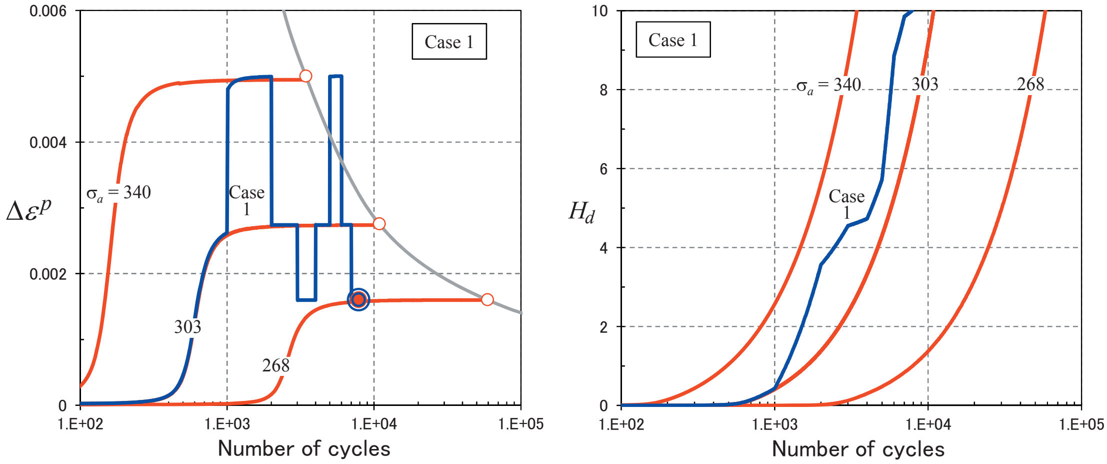

Fig.4 Evolution of plastic strain range and damage parameter H_d with the increase of number of cycles (Case 1)

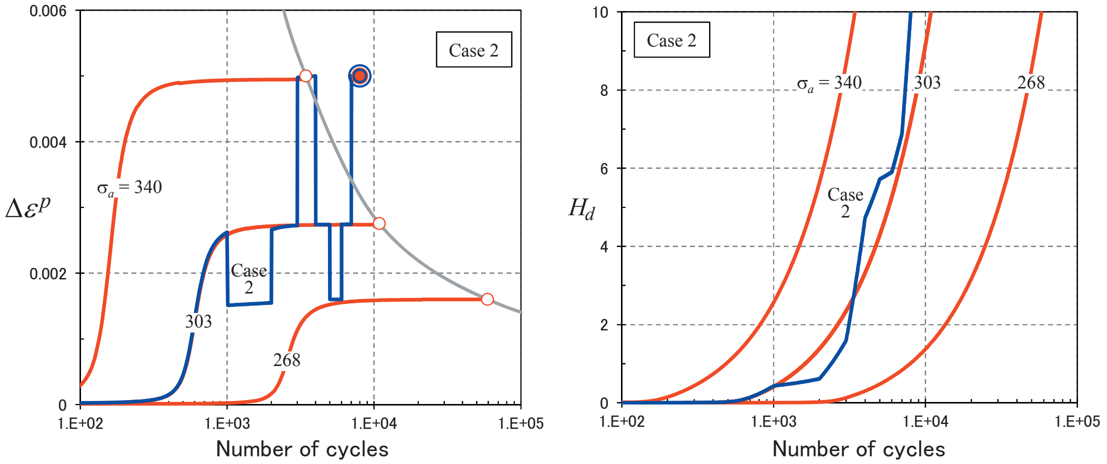

Fig.5 Evolution of plastic strain range and damage parameter H_d with the increase of number of cycles (Case 2)

with and without the periodic changes of applied stresses are examined.

The highlights of this model and the predicted results are summarized as follows.

1. The model incorporating subloading, elastic boundary and damage parameter describes a smooth elastic-plastic transition from macroscopically elastic to fully elastoplastic response.

2. Plastic strain is actualized after certain number of cycles, depending on the magnitude of the applied cyclic stresses under macroscopically elastic condition,

3. The elastic responses are described for the lower stress state than that of elastic boundary surface, whilst conventional model cannot.

4. The mechanical responses of the model with the damage counting parameter are examined with and without the periodic changes of applied stresses. Then it is found that the accumulation of damage depends highly on the applied stress and its histories.

The validity of the present model, however, should be confirmed by comparing with the experimental results on the stress-strain responses and life curves.

References

[1] Suresh S. Fatigue of materials, Cambridge Univ. Press, 1998.

[2] Toyosada M, Gotoh, K, Niwa T. Fatigue crack propagation for a through thickness crack: a crack propagation law considering cyclic plasticity near the crack tip, Int. J. Fatigue, Vol. 26, pp. 983-992, 2004.

[3] Mroz Z. On the description of anisotropic workhardening, J. Mech. Phys. Solids, Vol. 15, pp. 163-175, 1967.

[4] Dafalias Y.F., Popov, E.P. A model of nonlinearly hardening materials for complex loading, Acta Mech., Vol. 21, pp. 173-192, 1975.

[5] Dafalias Y.F., Herrmann, L.R. A bounding surface soil plasticity model, Proc. Int. Symp. Soils under Cyclic Trans. Load., Swansea, pp. 335-345, 1980.

[6] Hashiguchi K. Subloading surface model in unconventional plasticity, Int. J. Solid Struct., Vol. 25(8), pp. 917-945, 1989.

[7] Ohno N, Wang, J.-D. Kinematic hardening rules with critical state of dynamic recovery, part I: formation and basic features for ratcheting behavior, Int. J. Plasticity, Vol. 9(3), pp. 375-390, 1993.

[8] Hashiguchi K, Yoshimaru T. A generalized formulation of

the concept of nonhardening region, Int. J. Plasticity, Vol. 11(4), pp. 347-365, 1995.
[9] Drucker D.C. Conventional and unconventional plastic response and representation, Appl. Mech. Rev. (ASME), Vol. 41, pp. 151-167, 1988.
[10] Hashiguchi K, Chen Z.-P. Elastoplastic constitutive equation of soils with the subloading surface and the rotational hardening, Int. J. Numer. Anal. Meth. Geomech., Vol. 22, pp. 197-227, 1998.
[11] Hashiguchi K, Tsutsumi S. Elastoplastic constitutive equation with tangential stress rate effect, Int. J. Plasticity, Vol. 17(1), pp. 117-145, 2001.
[12] Tsutsumi S, Hashiguchi K. General non-proportional loading behavior of soils, Int. J. Plasticity, Vol. 21(10), pp. 1941-1969, 2005.
[13] Hashiguchi K, Tsutsumi S. Shear band formation analysis in soils by the subloading surface model with tangential stress rate effect, Int. J. Plasticity, Vol. 19(10), pp. 1651-1677, 2003.
[14] Hashiguchi K, Tsutsumi S. Gradient plasticity with the tangential subloading surface model and the prediction of shear band thickness of granular materials, Int. J. Plasticity, Vol. 23(5), pp.767-797, 2007.
[15] Tsutsumi S, Toyosada M, Hashiguchi K. Extended subloading surface model incorporating elastic boundary concept, J. Appl. Mech. (JSCE), Vol. 9, pp.455-462, 2006.
[16] Tsutsumi S. Cyclic and gradient plasticity model extended to fatigue and scale-dependent phenomena under macroscopically elastic condition, Doctor Thesis, Kyushu University, 2007.
[17] Tsutsumi, S., Murakami, K., Gotoh, K., Toyosada, M., Cyclic stress-strain relationship during high cycle fatigue process: elastoplastic constitutive model introducing cyclic damage effect, J. of the Japan Society of Naval Architects and Ocean Engineers, Vol.7, pp.243-250, 2008.